Published in final edited form as:
J Neurosci Methods. 2013 April 15; 214(2): 119–125. doi:10.1016/j.jneumeth.2013.01.020.

Sub-meninges Implantation Reduces Immune Response to Neural Implants

Neil T. Markwardt,
The University of Oklahoma, College of Engineering, Bioengineering Center, 202 W. Boyd St., Carson Eng. Ctr. Rm 107, Norman, OK 73019

Jodi Stokol, and
The University of Texas at Dallas, School of Behavioral and Brain Sciences, Erik Jonnson School of Engineering, 800 West Campbell GR41, Richardson TX 75080

Robert L. Rennaker II
The University of Texas at Dallas, School of Behavioral and Brain Sciences, Erik Jonnson School of Engineering, 800 West Campbell GR41, Richardson TX 75080

Abstract

Glial scar formation around neural interfaces inhibits their ability to acquire usable signals from the surrounding neurons. To improve neural recording performance, the inflammatory response and glial scarring must be minimized. Previous work has indicated that meningeally derived cells participate in the immune response, and it is possible that the meninges may grow down around the shank of a neural implant, contributing to the formation of the glial scar. This study examines whether the glial scar can be reduced by placing a neural probe completely below the meninges. Rats were implanted with sets of loose microwire implants placed either completely below the meninges or implanted conventionally with the upper end penetrating the meninges, but not attached to the skull. Histological analysis was performed 4 weeks following surgical implantation to evaluate the glial scar. Our results found that sub-meninges implants showed an average reduction in reactive astrocyte activity of 63% compared to trans-meninges implants. Microglial activity was also reduced for sub-meninges implants. These results suggest that techniques that isolate implants from the meninges offer the potential to reduce the encapsulation response which should improve chronic recording quality and stability.

Keywords

neural interface; microwire; meninges; glial scar; astrocyte; microglia

1. Introduction

The purpose of extracellular neural interfaces is to allow acquisition of neural signals with a high signal-to-noise ratio over a long period of time, in order to facilitate a wide range of therapeutic and research applications. Devices already in use provide relief from the symptoms of Parkinson's disease (Krack et al., 2003), restore hearing, or control a computer cursor or a robotic arm, in addition to allowing researchers to study neural processing

(Stieglitz et al., 2009). Future neural interfacing applications include restoration of function lost due to CNS disease or trauma, including blindness and paralysis, and chronic CNS mediated control of prosthetic devices (Polikov et al., 2005; Stieglitz et al., 2009). Significant advances have been made in the past 30 years towards developing a reliable cortical neural interface, but challenges still remain which prevent such technology from being clinically viable. Chief among these is the biocompatibility of the interface. Insertion of a recording implant into the cortex initiates short- and long-term inflammatory processes which can result in neuron death and eventual encapsulation and failure of the implant (Biran et al., 2005; Kalman, 2003; Turner et al., 1999). Numerous strategies have been employed to attempt to mitigate the brain's foreign body response, reduce encapsulation and minimize neuronal loss, improving recording performance. These strategies include alterations to the probe's size and shape, addition of drugs or polymers, and modification of the implantation procedure (Chen et al., 1997; Cui et al., 2003; He et al., 2006; Hsu et al., 2009; Rousche et al., 2001; Shain et al., 2003; Williams et al., 2005). The addition of a dexamethasone-eluting coating was found to help reduce the astrocytic response (Shain et al., 2003), but a coating of Parylene-C, often used in other medical device applications, did not affect the immune response (Winslow et al., 2010). Reduced implant size and elimination of conventional skull fixation have also been shown to reduce the immune response (Kim et al., 2004; Thelin et al., 2011). Despite the improvements that have been made, the majority of recording lifetimes for many different types of interfaces are still on the order of several months, far short of what is necessary for a clinically viable therapeutic interface (Merrill and Tresco, 2005; Polikov et al., 2005; Rennaker et al., 2005; Shain et al., 2003). Viable recordings have been acquired for as long as two to three years in some cases, but such extended lifetimes are generally rare (Simeral et al., 2011). One common aspect of current array technology which has not received significant attention is the basic dura-crossing design of conventional wired probes. Essentially all current neural interfaces consist of some kind of penetrating electrode spike or wire which is embedded in the cortical tissue and attached to a structure and wires on the surface of the cortex, which convey the signal out of the skull.

It has been suggested that some of the cells which participate in the immune response are derived from the meningeal space, in addition to the native astrocytes and microglia (Cui et al., 2003; Fawcett and Asher, 1999; Kalman, 2003; Maxwell et al., 1990; Ness and David, 1997). The development of methods to prevent these cells from migrating down the electrode might improve recording performance. In effect, meningeal cells and glial cells attempt to encapsulate a penetrating electrode in the same glia limitans which encapsulates the rest of the CNS (Fawcett and Asher, 1999). Rapid regrowth of the dura mater has been observed during the use of chronic neural recording chambers in primates, often interfering with recording procedures and illustrating the ability of meningeal tissue to respond quickly to injury (Arieli et al., 2002; Gray et al., 2007). The spatial relationship between the meningeal space and the implant has not yet been examined for its effects on the encapsulation response. A study using porous hollow fiber membrane implants showed relatively modest immune activity despite their large size compared to typical neural interfaces. It is possible that the immune response was minimized because of the porous nature of the implant, allowing meningeal cells to grow through the implant versus down the implant (Kim et al., 2004).

The current study directly examines the effect of trans-meningeal implantation on the chronic immune response to a neural implant. For ease of availability and ready comparison to current technologies, microwire segments were used in the current study in two implantation configurations, conventionally (trans-meninges) and sub-meninges, in the rat cortex for a period of four weeks, and brain sections were subjected to quantitative immunohistochemistry analysis.

2. Materials and Methods

2.1 Subjects

Ten male Long Evans rats were individually housed in a temperature- and humidity-controlled environment and were exposed to a 12:12 h light-to-dark cycle with free access to food and water.

2.2 Implants

Implants for this study consisted of individual lengths of 50μm diameter stainless steel microwire with a polyimide coating. This is similar to materials which have been used to construct microwire recording arrays (Nicolelis et al., 2003; Williams et al., 1999). Each animal received three sub-meninges implants and three trans-meninges implants. To ensure consistent implantation depth, insertion of the microwire implants was performed using a mechanical insertion device. The insertion device consisted of a 25 gauge needle with a plunger wire inside the needle and the device was mounted to a micromanipulator. To perform an insertion, a microwire segment which has been sonicated in ethanol and rinsed with sterile saline is inserted into the end of the inserter needle with the plunger retracted, then the assembly is lowered, bringing the tip of the implant into contact with the cortical surface. The inserter is then lowered to allow the implant and needle tip to incise the dura. The plunger is then depressed to push the implant out of the end of the inserter needle into the cortical tissue. Two different plunger lengths are used for the two implantation types – sub-meninges implants are accomplished using a plunger which extends to the end of the needle tip when depressed, forcing the implant ~200μm below the cortical surface. Trans-meninges implants utilize a shorter plunger which leaves the end of the implant ~200μm above the cortical surface. A diagram of the insertion device and the two implant types is shown in Fig 1. Implant lengths were chosen to yield a consistent implantation depth of 2mm for the lower end of both implant types, so submeningeal implants were ~1.8mm in length and transmeningeal implants were ~2.2mm.

2.3 Surgical Procedures

Surgical procedures are similar to those reported previously (Rennaker et al., 2005). Briefly, rats were anesthetized using ketamine, xylazine and acepromazine (targeted dosage 50, 20, 5 mg/kg respectively). A midline incision was made in the scalp and the connective tissue was dissected from the skull. Two bone screws were implanted into the left side of the skull to secure the acrylic skull cap. A 3 mm × 5 mm portion of the right parietal bone was removed using micro-rongeurs. Three microwire implants of each treatment were inserted in the manner described above. All subjects received both implant types in order to minimize the effects of animal-to-animal variability. Following implantation, the brain was covered by a layer of silicone elastomer (Kwik-Cast; World Precision Instruments, Inc., FL) and a layer of acrylic was added to seal the craniotomy and secure the structure to the bone screws. The initial incision was closed using absorbable sutures.

2.4 Immunohistochemistry

At 4 weeks post-implantation, subjects were euthanized and perfused. Subjects were administered 0.7 mL of the same ketamine cocktail used for the surgical procedure, and then transcardially perfused with 100 mL of phosphate buffered saline (PBS) followed by 100mL of 4% paraformaldehyde in PBS. The brain was removed and stored (4°C) for 48 h immersed in a solution of 30% sucrose by volume and 4% paraformaldehyde for postfixation and cryoprotection. Both sub- and trans-meninges implants were still in the brain following removal of the skull. These wires were removed from the brain prior to and during blocking of tissue around the implant site for sectioning. The brain was cut into 40μm

thick horizontal sections which were collected free-floating in PBS. Alternating sections were stained with antibodies for GFAP to label activated astrocytes, and IBA1 to label activated microglia in both phagocytic and nonphagocytic forms (Jones and Tuszynski, 2002; Nakajima and Kohsaka, 2001; Polikov et al., 2005). All sections were also labeled with NF160 anti-neurofilament antibody to visualize neuronal processes surrounding the tracks. Following three washes in PBS, sections were blocked in 3% normal donkey serum for 30 minutes. Sections were then incubated overnight in primary antibody solutions (NF160 and GFAP or IBA-1, 1:250) in a buffer containing 3% normal donkey serum and 0.3% Triton X-100. The following day, sections were incubated in secondary antibodies for 2h and then visualized with AlexaFluor 555 (Invitrogen) and coverslipped using Vectashield with DAPI (Vector Laboratories). All tissue sections in this study were stained at the same time with the same primary and secondary solutions to ensure consistency. Images were taken using an Olympus BH-2 microscope with a 10× objective and an Olympus DP70 digital camera.

2.5 Analysis

Images were analyzed using ImageJ software (NIH) to perform automated thresholding and area measurements of the activated regions surrounding electrode tracks for GFAP labeled images. Contralateral control sections were used to determine average background fluorescence levels and set threshold values for each cell type for each animal. Pixel count was converted to square microns of activated area around each track. An example track is shown in Fig 2 with the above-threshold region outlined to illustrate the area that was measured. Due to the nature of the cells, IBA1 labeled images could not be subjected to the same simple area measurement method as GFAP images. Instead, a radial intensity profile function in ImageJ was used to measure the average fluorescence intensity as a function of radius from the implant-tissue interface. These intensity integrals, consisting of the area under the intensity curve, were then separated into 6 bins of 50μm each for statistical analysis. The same radial intensity profile technique was also used to examine GFAP labeled activity. For all analyses except for depth comparisons, a single mean intensity or area value was found for each track across all section depths.

3. Results

3.1 Astrocyte activity

Fluorescent labeling with antibodies for glial fibrillary acidic protein (GFAP) was used to identify reactive astrocytes. GFAP labeled images exhibited regions of reactive astrocyte activity surrounding each implant track, forming a densely packed, multilayered capsule which is typical of a neural implant at a 4 week time point.

3.1.1 Morphology—Morphology of GFAP+ cells was consistent with that of reactive astrocytes in the CNS. The GFAP+ sheath surrounding each implant track was accompanied by a surrounding area of GFAP+ cells extending tens to a few hundred microns from the implant center in a generally radially symmetric fashion. The GFAP+ regions surrounding the tracks were clearly delineated from the surrounding background, allowing the use of simple threshold-based software to determine the regions' size.

Figure 3 shows two example images from a single tissue section stained for GFAP. The sub-meninges implant (A) and trans-meninges implant (B) are shown side by side for comparison. This representative sample illustrates the dramatic difference in GFAP expression between the two implantation methods.

3.1.2 Quantitative GFAP measures—The areas for each section were measured using Image-J. Sub-meninges implants showed 63% less GFAP labeled cellular area on average than trans-meninges implants, as shown in Figure 3C (t-test, n=30, $p<0.001$).

A previous study (Thelin et al., 2011) found that implants tethered to the skull tended to form larger cavities that were elongated in the rostral-caudal axis. It is possible that the trans-meninges implants in the current study were mechanically attached to the silicone used to cover the brain following implantation. This is unlikely given that we removed the wires from the brain after the skull was detached. The silicone came off with the skull in most cases.

If the trans-meninges implants were attached to the silicone, it is likely that an asymmetry in the wound site or GFAP response would be present due to relative motion between the brain and the skull. An examination of the voids at the center of the GFAP labeled areas found no differences in void area between implant types (t-test, $p = 0.76$). Measurement of the voids' edge-to-edge distances in the rostral-caudal (y) and medial-lateral (x) directions revealed no significant elongation of the voids along either axis for either sub-meninges ($p=0.47$) or trans-meninges implants ($p=0.75$), as shown in Figure 4. This scatter plot reveals a general grouping of the data around the line y=x, which indicates a circular void, and suggests that the trans-meninges implants were not tethered to the skull.

The same images were also subjected to analysis via radial intensity profiling, in order to measure the fluorescence intensity as a function of distance from the implant-tissue interface and examine the spatial distribution of the astrocyte response. It was found that sub-meninges implants taken from the same cortical slice had significantly less GFAP labeled cellular activity out to a radius of 300 microns (Figure 5). The intensity profile analysis illustrates both the reduced intensity and reduced radial extent of reactive astrocyte activity for sub-meninges implants. The general scale of the astrocyte response is consistent with other histological studies using implants of this general size (Biran et al., 2005; Winslow and Tresco, 2010). Due to imaging constraints and the proximity of neighboring tracks and section edges, we could not measure fluorescence intensity consistently any further than 300μm for the entire data set, therefore the measurements at 350μm are from a subset of about 1/2 of all tracks. For this radius bin, though, no difference in integrated intensity was found between the two implant types (t-test, $p = 0.057$). This indicates that GFAP+ reactivity has returned to background levels at 350μm from the implant surface for trans-meninges implants. ANOVA comparison of the radius bins for sub-meninges implants showed no difference between the 250, 300 and 350μm radii, indicating that GFAP+ activity has returned to background levels at a 250μm radius for the sub-meninges implants. Thus, the typical maximum extent of reactive astrocyte activity is reduced by about 100μm by sub-meninges implantation.

3.1.3 Astrocyte activity by section depth—In addition to examining mean track areas across all section depths to compare sub-meninges and trans-meninges implants, GFAP area data were grouped and analyzed according to section depth in order to better understand the spatial distribution of the astrocyte response. A subset of coronal sections as shown in figure 2 using trans-meninges microwire implants exhibited decreasing GFAP+ activity with increasing depth down the electrode track. It was this anecdotal evidence that in-part motivated the current study. If the meningeal tissue were growing down the shaft, it is reasonable to assume that at early stages in the immune response the glial scar would be larger at the more superficial layers. When the data from this study are arranged by depth, no such trend is evident (Fig 6). Neither type of implant shows statistically significant differences in astrocyte activity between section depths. It is likely that the elevated response near the cortical surface was not captured because we only compared sections in

which both sub and trans-meninges implants were present (>200μm below the cortical surface). The topmost layers of the cortex were not collected due to the lack of chronic sub-meninges implant tracks. Additionally, it is possible that any cellular migration from the cortical surface is already complete by the 4 week time point employed in this study.

3.2 Microglia activity

Adjacent sections utilized IBA1 antibodies to label activated microglial cells, and these also showed a region of cellular activity immediately surrounding the implant. Cellular morphology was consistent with that of activated microglial cells. IBA1+ regions were much smaller than GFAP+ regions for the same tracks, which is consistent with other findings that microglial activity peaks in the first week post-injury and astrocyte activity dominates from then on (Biran et al., 2005; Polikov et al., 2005). Representative IBA1 labeled images from the same tissue section for sub-meninges and trans-meninges implant tracks are shown in Fig 7A and B, respectively. Due to the sometimes more diffuse nature of the microglial cellular activity, intensity profiling was used exclusively for analysis rather than area measurements. IBA1 labeled sections showed statistically significant reductions in fluorescence intensity for the first three radius bins of 0–150μm from the implant surface (t-test, $p<.05$), as shown in Fig 7C. There were no significant differences in IBA1 reactivity for sub-meninges or trans-meninges implants at radii greater than 200μm from the center of the electrode track.

Both the mean intensity and the radial extent of microglia cellular activity were reduced by sub-meninges implantation. Combined with the reduction in reactive astrocyte activity, this constitutes a large reduction in the size and scope of the foreign body response for sub-meninges implants, which should correspond to an improvement in recording array performance for sub-meningeally implanted recording devices.

As with GFAP sections, no significant trend was found when IBA1 fluorescence intensity values for the significant radius bins were compared according to section depth (data not shown). Given that a greater degree of variability was found in IBA1 labeled activity than with GFAP, a subtle trend in reactivity with depth is more difficult to separate from normal variation.

3.3 Neurofilament results

Visualization of neuronal processes using NF160 antibody labeling did not produce sufficiently consistent results for meaningful data to be obtained. Morphology of labeled structures was consistent with neuronal processes, indicating proper function of the antibody, but the degree of labeling exhibited a high degree of variability from track to track and section to section not seen with the other techniques used in this study. Some implant tracks exhibited areas of elevated NF160 expression immediately surrounding the track. An increase in neuronal density immediately surrounding a track is not consistent with widely observed neuronal dieoff surrounding an implant (Biran et al., 2005; Turner et al., 1999; Winslow and Tresco, 2010), but a similar phenomenon has been observed by other researchers when using the NF160 antibody (Winslow and Tresco, 2010). Future studies will employ NeuN to label neuron cell bodies and better allow quantification of viable neurons around the implant site.

4. Discussion

The results of this study suggest that the meninges play a role in determining the extent of the immune response at 4 weeks post-implantation. The data demonstrate that the immune response to a cortical implant is greatly reduced when the entire implant is not in contact

with the meninges. The average amount of GFAP-labeled cellular activity, which is the primary metric of the chronic immune response (Kalman, 2003; Polikov et al., 2005; Szarowski et al., 2003; Turner et al., 1999), was nearly threefold greater for trans-meninges implants than sub-meninges implants (Fig 3C). As fibrous encapsulation by reactive astrocytes has been shown to be strongly correlated with neural recording device failure, this reduction should correspond to an improvement in recording device performance and signal lifetime (Polikov et al., 2005).

Radial intensity profile analysis was also used to examine the astrocyte response. This revealed a reduction in both the intensity and the extent of GFAP labeled cells surrounding sub-meninges implant tracks. GFAP intensity was significantly reduced for all 6 radius bins that were measured out to a distance of 300 microns from the implant-tissue interface (Fig 5). At 350μm, GFAP intensity had returned to the background level. The greatest reductions in integrated fluorescence intensity were seen in the 150μm and 200μm radius bins, indicating a reduction in the overall extent of the astrocyte response in addition to the intensity reduction. This is consistent with the findings of the threshold-based area measurements. The reduction of mean astrocyte activity in this 100 micron radius zone is particularly important for neural interface function, since this is thought to be the maximum radius from which neural signals may be acquired, and elevated GFAP+ activity has been shown to be negatively correlated with neuron viability (Biran et al., 2005; Henze et al., 2000; Winslow and Tresco, 2010).

A reduction was also seen in areas of IBA1 labeled microglial activity. Microglial cell activity tends to peak around 1 week post-injury (Biran et al., 2005; Kalman, 2003; Polikov et al., 2005) and is reduced from its peak level by the 4 week time point used in this study, but a thin sheath of activated cells still surrounds each implant track, in the same region as the activated astrocytes. As microglia participate primarily in the acute inflammatory phase of the immune response and their activity should have decreased significantly by the 4 week time point used in this study, (Biran et al., 2005; Kreutzberg, 1996; Nakajima and Kohsaka, 2001; Polikov et al., 2005) the observed reduction in microglial activity indicates that sub-meningeal implantation likely has desirable effects on the acute phase of the immune response in addition to the chronic phase, which is characterized mainly by reactive astrocyte activity and the formation of the glial scar (Carbonell and Boya, 1988; Kalman, 2003). The reduction of microglial activity is also likely to have a desirable effect on neuronal viability in the region surrounding the implant, as the presence of these cells has been correlated with neuronal death (Biran et al., 2005). This may be mediated directly by a number of cytotoxic compounds that have been shown to be secreted by microglia which cause neuron death or alteration of function, including monocyte chemotactic protein-1 (MCP-1) and tumor necrosis factor-alpha (TNF-α), among numerous others (Biran et al., 2005). The presence of IBA1+ cells in the immediate vicinity of the implant may suggest the existence of a persistent inflammatory state, based on findings that such cellular reactions are only found in the case of indwelling implants, and not in the case of stab wounds (Biran et al., 2005). Given the observed decrease in IBA1 immunoreactivity for sub-meninges implants in the current study, it seems likely that a reduction in chronic inflammatory activation makes up some part of the mechanism responsible.

The mechanisms which may account for the observed reduction in the foreign body response due to sub-meningeal implantation are not fully understood, but there are some factors which are thought to contribute to the immune response which may be affected by the implant's location. Meningeally derived fibroblasts have been found to migrate into the wound from the meningeal space and contribute to the inflammatory response (Kalman, 2003; Kim et al., 2004; Maxwell et al., 1990; Ness and David, 1997), and positioning the implant below the cortical surface may reduce this component. In one study, an

encapsulating sheath of meningeal fibroblast cells was found surrounding silicon "Michigan" probes implanted in the guinea pig cortex at two weeks (Cui et al., 2003). In effect, these cells participate along with reactive astrocytes in the process of forming a new glia limitans around the implant which migrates down the wound track from the pial surface (Maxwell et al., 1990). Sub-meningeal implantation of the device physically removes it from the pial space, and thus likely inhibits this process.

Placement of the implant below the meninges may reduce chronic micromotion between the implant and the surrounding cortical tissue, which has been implicated in exacerbating the chronic immune response. It has been shown that hollow fiber membrane cortical implants that were free-floating in the cortical tissue had reduced chronic immune activity compared to implants which were anchored to the skull (Kim et al., 2004). It is possible that the reactive cells grew through the membrane and not down the membrane. This suggests that an electrode with a porous substrate at the meninges might reduce the immune response. In the current study, available surgical techniques make it impossible to completely isolate the effects of implant location and chronic micromotion, as the upper ends of the trans-meninges implants are still in contact with the silicone elastomer used to seal the craniotomy. The amount of interface is small, though, and much softer than the fixation materials which have been employed for tethered implants to study this effect (Kim et al., 2004; Thelin et al., 2011). Also, the effects of tethered implantation, namely enlarged, elongated void areas (Thelin et al., 2011), were not present for either implant type in the present study. Figure 4 shows the distribution of track void dimensions along the rostral-caudal and medial-lateral axes, showing no void elongation or enlargement for either type of implant. Thus, it seems safe to conclude that chronic micromotion between the brain and implant did not play a large role in producing the observed difference between the implant types.

These results provide insight into a potential method to significantly reduce the glial reaction to intracortical electrodes, but current technology does not provide an easy way to realize those improvements with a functional recording device. Wireless neural recording devices are an area of much current interest, but existing devices rely on power and data transmission hardware which cannot be placed below the cortical surface, meaning that some part of the device must still cross the meninges (Bashirullah, 2010). As it seems likely that ingrowth of meningeal cells contributes significantly to the glial response, future work should pursue strategies which either miniaturize wireless implants such that the entire device may be placed sub-meningeally or discourage growth of meningeal cells down the penetrating elements. Other findings have suggested that porous implant structures may encourage meningeal tissue to grow into the implant rather than down the length of the shaft (Kim et al., 2004). Alginate dural sealants have seen limited use in conjunction with intracortical implants (Nunamaker and Kipke, 2010), but the potential effects of dural sealants on meningeal ingrowth and the glial response remain uninvestigated. It is hoped that future work will allow one of these or other methods to take advantage of the reduction in the glial reaction afforded by sub-meninges implantation.

5. Conclusions

Quantification of glial cell activity surrounding sub-meninges and trans-meninges microwire implants revealed that sub-meninges implantation yields a substantial decrease in the chronic immune response to a microwire implant. Subdural implantation of microwire segments produced an average reduction in astrocyte activity of 63% compared to conventionally implanted controls. Microglial activity was also reduced. This offers insight into the factors that govern the brain’s response to a neural implant, and these results also

suggest that techniques which isolate implants from the meninges may reduce the encapsulation response and improve chronic recording quality.

Acknowledgments

This work was funded by NIH NINDS R01NS62065

References

Arieli A, Grinvald A, Slovin H. Dural substitute for long-term imaging of cortical activity in behaving monkeys and its clinical implications. J. Neurosci. Meth. 2002; 114:119–133.

Bashirullah R. Wireless Implants. IEEE Microwave Mag. 2010:S14–S23.

Biran R, Martin DC, Tresco PA. Neuronal cell loss accompanies the brain tissue response to chronically implanted silicon microelectrode arrays. Exp. Neurology. 2005; 195:115–126.

Carbonell AL, Boya J. Ultrastructural study on meningeal regeneration and meningo-glial relationships after cerebral stab wound in the adult rat. Brain Res. 1988:337–344. [PubMed: 3359193]

Chen J, Wise KD, Hetke JF, Bledsoe SC. A multichannel neural probe for selective chemical delivery at the cellular level. IEEE Trans. on Biomed. Eng. 1997; 44:760–769.

Cui X, Wiler J, Dzaman M, Altschuler R, Martin DC. In vivo studies of polypyrrole/peptide coated neural probes. Biomaterials. 2003; 24:777–787. [PubMed: 12485796]

Fawcett JW, Asher RA. The glial scar and central nervous system repair. Brain Res. Bul. 1999; 49:377–391.

Gray CM, Goodell B, Lear A. Multichannel micromanipulator and chamber system for recording multineuronal activity in alert, non-human primates. J. Neurophysiol. 2007; 98:527–536. [PubMed: 17493924]

He W, McConnell GC, Bellamkonda RV. Nanoscale laminin coating modulates cortical scarring response around implanted silicon microelectrode arrays. J. Neural Eng. 2006; 3:316–326. [PubMed: 17124336]

Henze DA, Borhegyi Z, Csicsvari J, Mamiya A, Harris KD, Buzsaki G. Intracellular features predicted by extracellular recordings in the hipppocampus in vivo. J. Neurophysiol. 2000; 84:390–400. [PubMed: 10899213]

Hsu J, Rieth L, Normann RA, Tathireddy P, Solzbacher F. Encapsulation of an integrated neural interface device with parylene c. IEEe Trans. Biomed. Eng. 2009; 56:23–29. [PubMed: 19224715]

Jones LL, Tuszynski MH. Spinal cord injury elicits expression of keratan sulfate proteoglycans by macrophages, reactive microglia, and oligodendrocyte precursors. J. Neurosci. 2002; 22:4611–4624. [PubMed: 12040068]

Kalman M. Glial reaction and reactive glia. Adv. in Molec. and Cell Biol. 2003; 31:787–835.

Kim Y-T, Hitchcock RW, Bridge MJ, Tresco PA. Chronic response of adult rat brain tissue to implants anchored to the skull. Biomaterials. 2004; 25:2229–2237. [PubMed: 14741588]

Krack P, Chabardes S, Koudsie A, Benazzouz A, Benabid A. Five-year follow-up of bilateral stimulation of the subthalamic nucleus in advanced parkinson's disease. N. Engl. J. Med. 2003; 349:1925–1934. [PubMed: 14614167]

Kreutzberg GW. Microglia: a sensor for pathological events in the CNS. Trends Neurosci. 1996; 19:312–318. [PubMed: 8843599]

Maxwell WL, Follows R, Ashhurst DE, Berry M. The respopnse of the cerebreal hemisphere of the rat to injury 1. The mature rat. Phil. Trans. R. Soc. Lond. 1990; 328:479–500. [PubMed: 1974074]

Merrill DR, Tresco PA. Impedance characterization of microarray recording electrodes in vitro. IEEE Trans. on Biomed. Eng. 2005; 52:1960–1965.

Nakajima K, Kohsaka S. Microglia: activation and their significance in the central nervous system. J. Biochem. 2001; 130:169–175. [PubMed: 11481032]

Ness R, David S. Leptomeningeal cells modulate the neurite growth promoting properties of astrocytes in vitro. Glia. 1997; 19:47–57. [PubMed: 8989567]

Nicolelis MAL, Dimitrov D, Carmena JM, Crist R, Lehew G, Kralik JD, Wise SP. Chronic, multisite, multielectrode recordings in macaque monkeys. Proc. Nat. Acad. Sci. 2003; 100:11041–11046. [PubMed: 12960378]

Nunamaker EA, Kipke DR. An alginate hydrogel dura mater replacement for use with intracortical electrodes. J. Biomed. Materials Res. B. 2010; 95B:421–429.

Polikov VS, Tresco PA, Reichert WM. Response of brain tissue to chronically implanted neural electrodes. J. Neurosci. Meth. 2005; 148:1–18.

Rennaker RL, Street S, Ruyle AM, Sloan AM. A comparison of chonic multi-channel cortical implantation techniques: manual versus mechanical insertion. J. Neurosci. Meth. 2005; 142:169–176.

Rousche PJ, Pellinen DS, Pivin DP, Williams JC, Vetter RJ, Kipke DR. Flexible polyimide-based intracortical electrode arrays with bioactive capability. IEEE Trans. on Biomed. Eng. 2001; 48:361–371.

Shain W, Spataro L, Dilgen J, Haverstick K, Retterer S, Isaacson M, Saltzman M, Turner JN. Controlling cellular reactive responses around neural prosthetic devices using peripheral and local intervention strategies. IEEE Trans. Neural Sys. Rehab. Eng. 2003; 11:186–188.

Simeral JD, Kim S-P, Black MJ, Donoghue JP, Hochberg LR. Neural control of cursor trajectory and click by a human with tetraplegia 1000 days after implant of an intracortical microelectrode array. J. Neural Eng. 2011; 8:1–24.

Stieglitz T, Rubehn B, Henle C, Kisban S, Herwik S, Ruther P, Schuettler M. Brain-computer interfaces: an overview of the hardware to record neural signals from the cortex. Prog. Brain Res. 2009; 175:297–315. [PubMed: 19660664]

Szarowski DH, Andersen MD, Retterer S, Spence AJ, Isaacson M, Craighead HG, Turner JN, Shain W. Brain responses to micro-machined silicon devices. Brain Res. 2003; 983:23–35. [PubMed: 12914963]

Thelin J, Jorntell H, Psouni E, Garwicz M, Schouenborg J, Danielsen N, Linsmeier CE. Implant size and fixation mode strongly influence tissue reactions in the CNS. Pub. Lib. Sci. One. 2011; 6:e16267.

Turner JN, Shain W, Szarowski DH, Andersen MD, Martins S, Isaacson M, Craighead HG. Cerebral astrocyte response to micromachined silicon implants. Exp. Neurology. 1999; 156:33–49.

Williams JC, Holecko MM, Massia SP, Rousche PJ, Kipke DR. Multi-site incorporation of bioactive matricies into MEMS-based neural probes. J. Neural Eng. 2005; 2:L23–L28. [PubMed: 16317225]

Williams JC, Rennaker RL, Kipke DR. Long-term neural recording characteristics of wire microelectrode arrays implanted in cerebral cortex. Brain Res. Prot. 1999; 4:303–313.

Winslow BD, Christensen MB, Yang WK, Solzbacher F, Tresco PA. A comparison of the tissue response to chronically implanted parylene-c-coated and uncoated planar silicon microelectrode arrays in rat cortex. Biomaterials. 2010; 31:9163–9172. [PubMed: 20561678]

Winslow BD, Tresco PA. Quantitative analysis of the tissue response to chronically implanted microwire electrodes in rat cortex. Biomaterials. 2010; 31:1558–1567. [PubMed: 19963267]

- We implanted microwires in rat cortex crossing and entirely below the meninges
- Sub-meninges implants showed 63% less astrocyte activity
- Sub-meninges implantation also reduced the microglial reaction

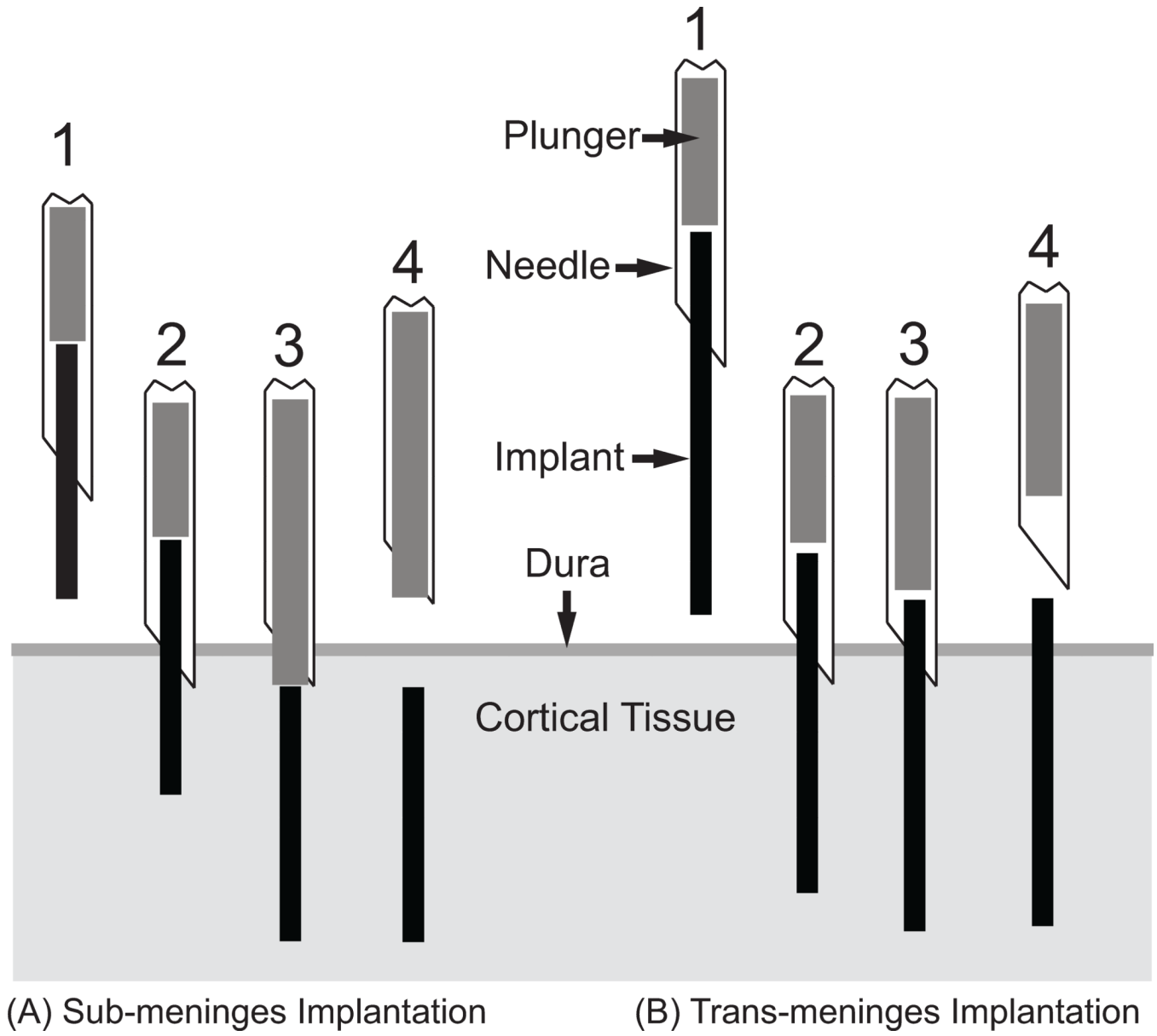

Fig 1.

Implantation Scheme - Needle loaded with implant is positioned above implant site (1).
Tip of implant and needle are lowered into cortical tissue$_{[0]}$ through the dura (2).
Plunger is depressed, pushing implant into tissue (3).
Needle is retracted, leaving implant in place (4).
Sub-meninges probes are placed approximately 200μm below the cortical surface.

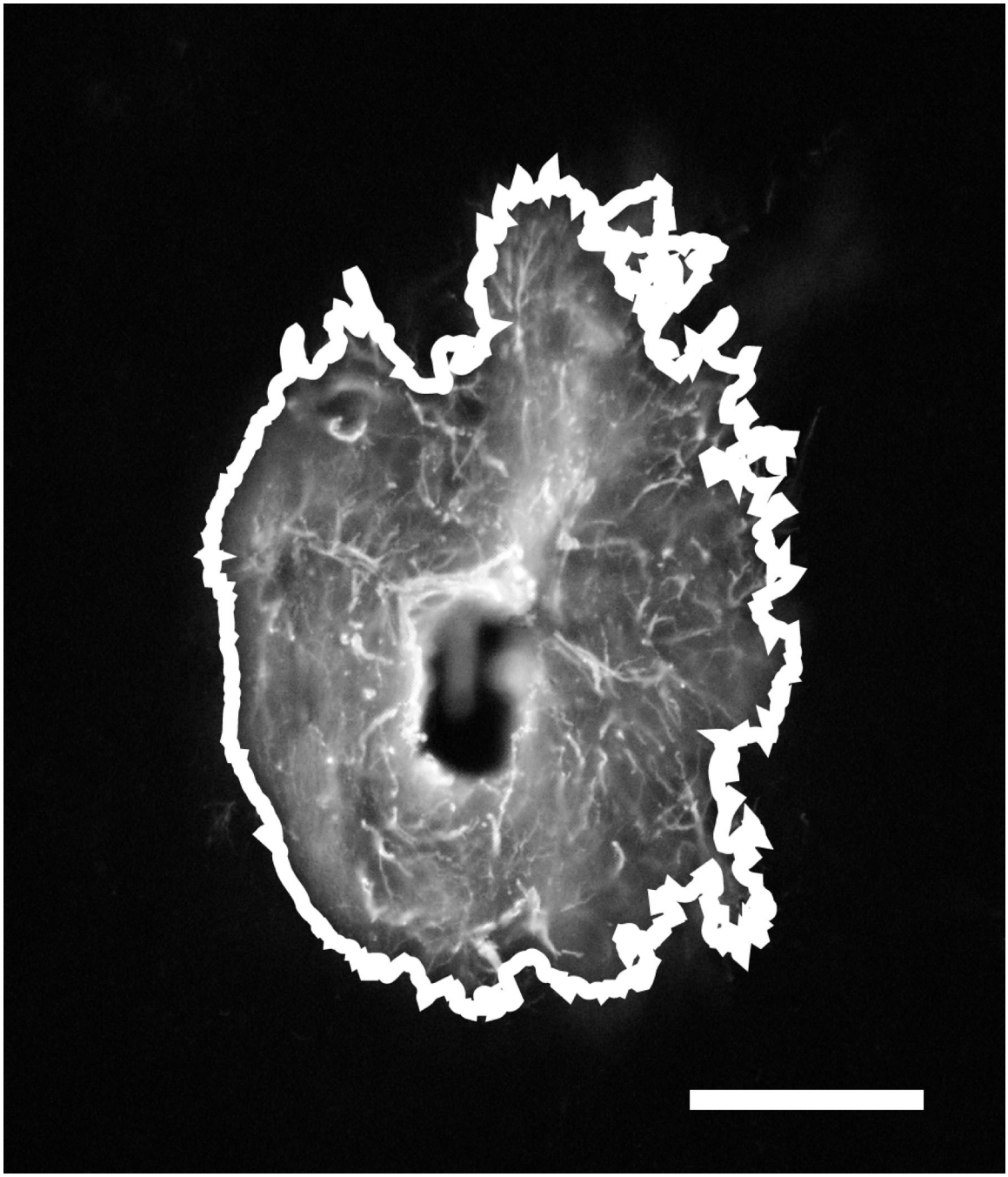

Fig 2.
Typical GFAP labeled trans-meninges implant track showing area count border generated by ImageJ. Scale bar = 100μm.

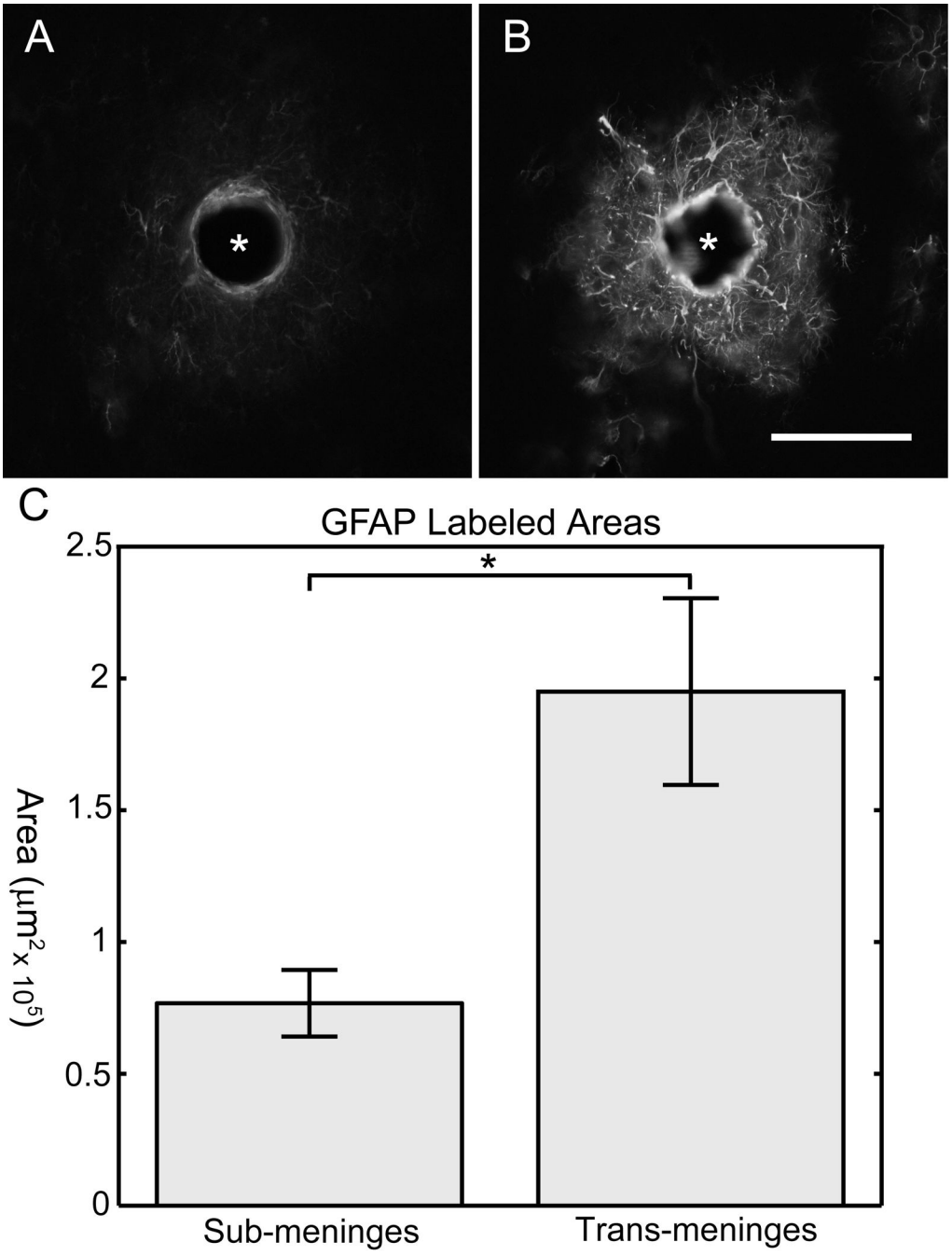

Fig 3.
GFAP Results
Sub-meninges implant track (A) and trans-meninges implant track (B) from the same tissue section. Scale bar = 100μm (* denotes implant location)
C) Mean GFAP labeled track areas for sub-meninges and trans-meninges implants +/− 95%CI (*p<.001)

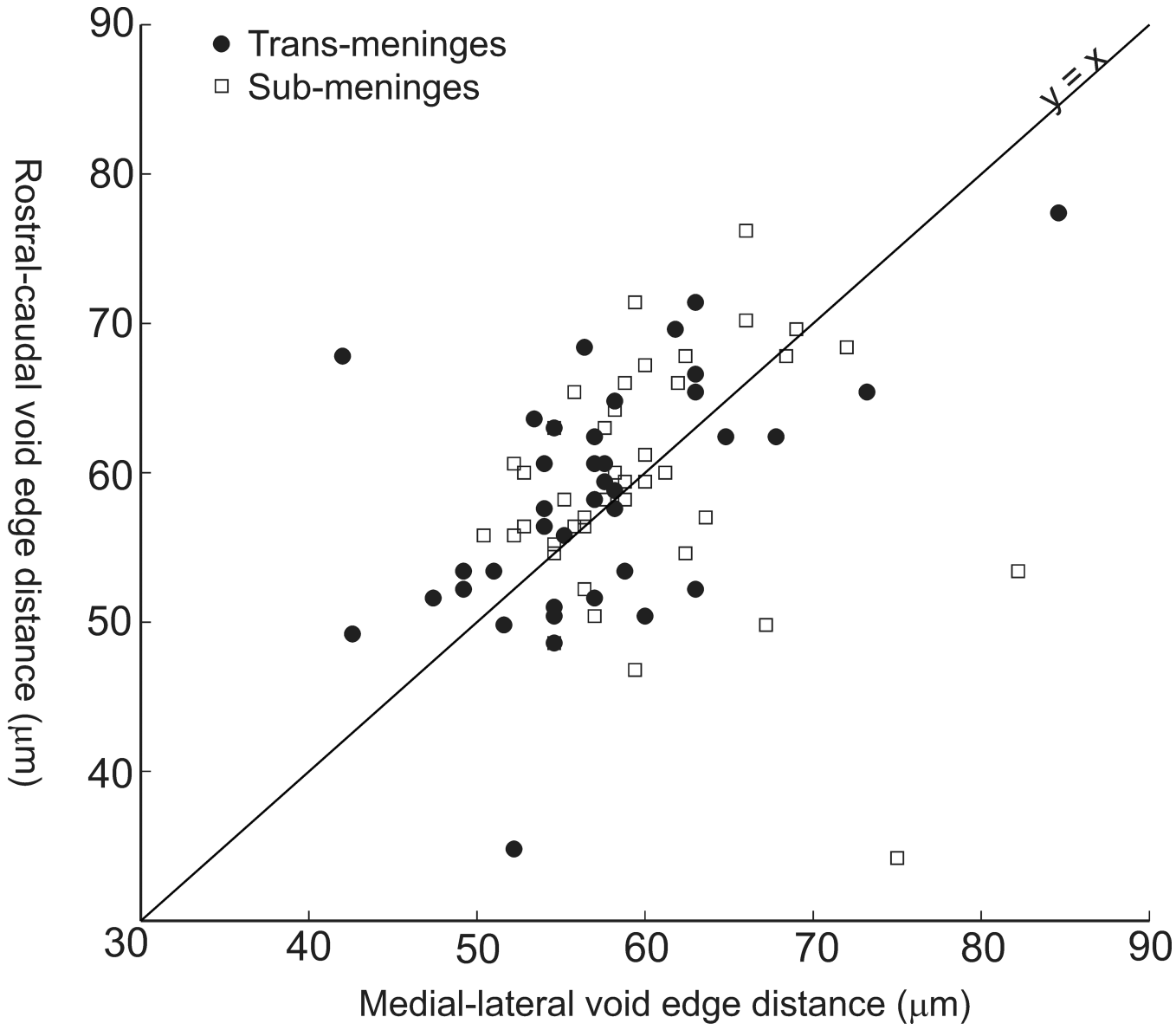

Fig 4.
Edge-to-edge dimensions of track voids for both implant types showing data from deepest and shallowest sections only. Line (y=x) indicates no void elongation in either direction.

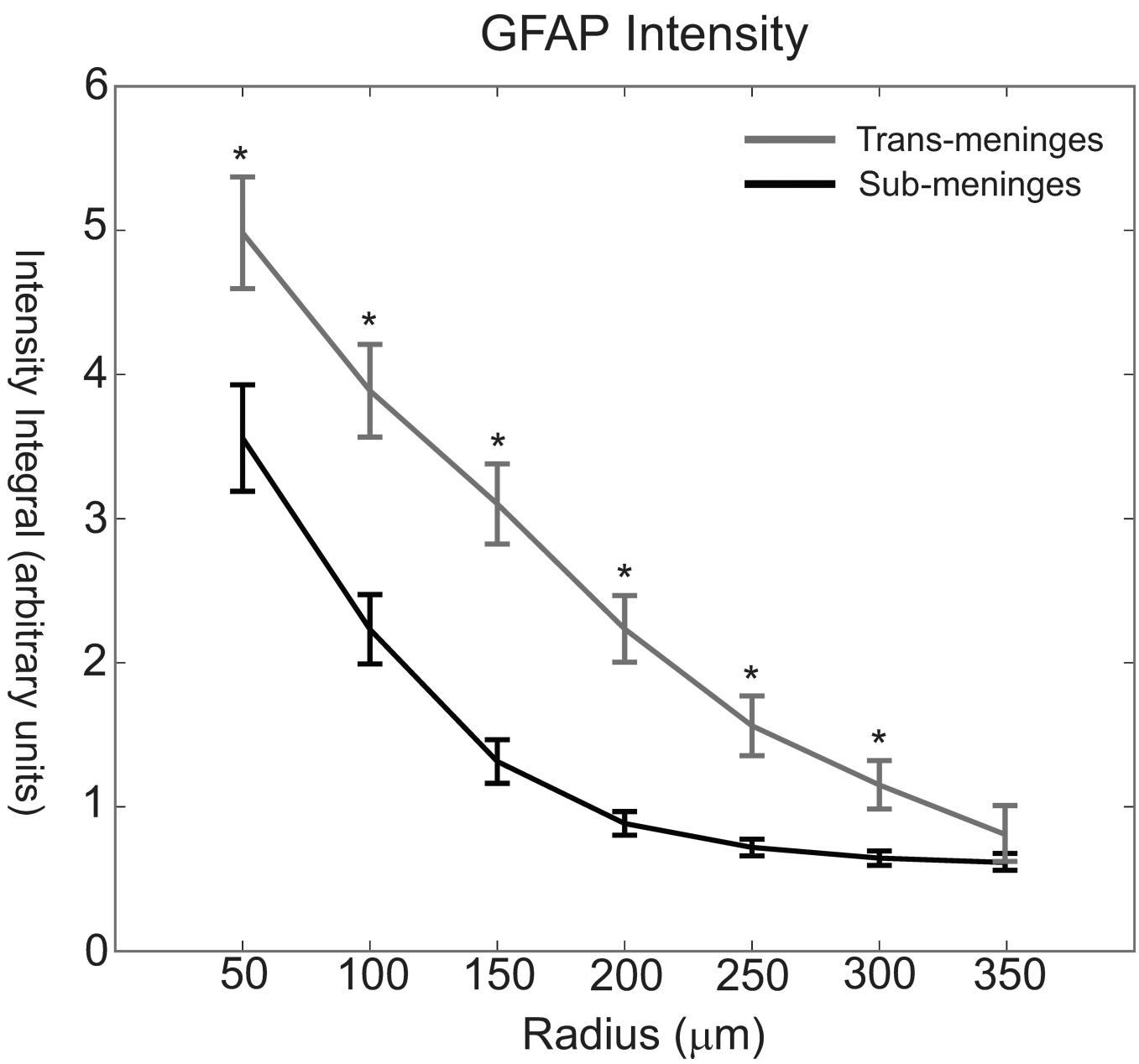

Fig 5.
GFAP intensity as a function of radius for trans-meninges[0] and sub-meninges implants +/− 95%CI (*p<.001)

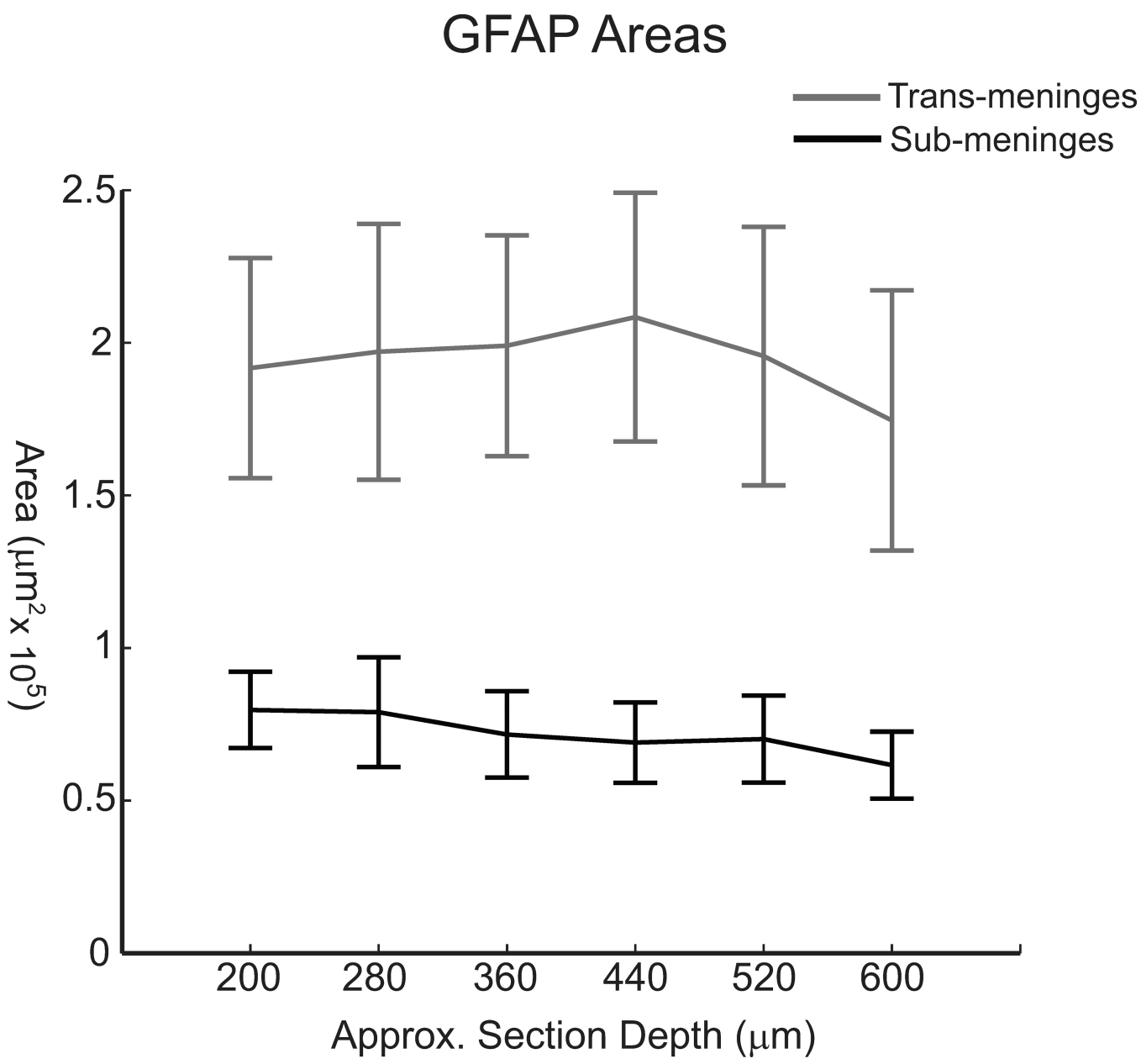

Fig 6.
Mean GFAP labeled areas grouped by section depth for sub-meninges and trans-meninges implants

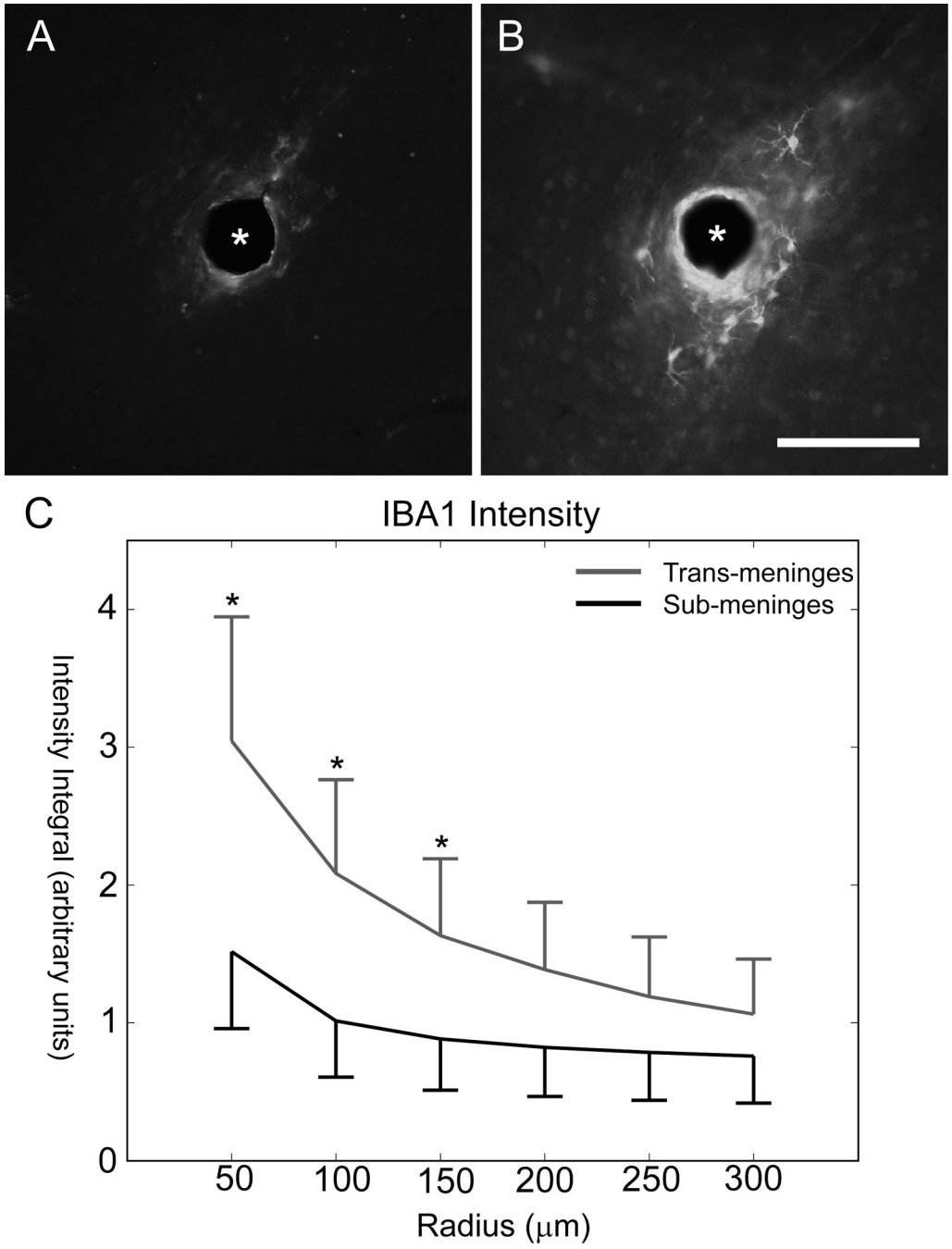

Fig 7.
IBA1 Results
Sub-meninges implant track (A) and trans-meninges implant track (B) from the same tissue section (scale bar = 100μm)
C) IBA1 intensity as a function$_{[0]}$ of radius for sub-meninges and trans-meninges implants +/− 95% CI (*$p<0.05$)